the limit of zero external transverse field (*16*). For our dilute crystals, the net outcome is neither a ferromagnetic nor a spin-glass ground state (*17*, *18*) but instead a subdivision of the system into clusters, whose conventional freezing is eventually limited by the quantum fluctuations brought about by the transverse fields from other clusters. The coherent oscillations that we observe could then be thought of as Rabi oscillations of the clusters in the weak transverse mixing fields.

We can use our data to see the crossover to quantum behavior and to measure the size of the clusters. The classical-quantum crossover is apparent from plotting (Fig. 1, inset) the frequency f_p where the imaginary part of the magnetic response peaks against temperature. At high T a thermally activated Arrhenius form, $f_p \sim \exp(-\Delta/k_BT)$, fits the data with a barrier height $\Delta = 1.2$ K $\sim J_{nn}$. For $T < 0.120$ K, the sharp gap-like cutoff appears in $\chi''(f)$ and there is a clear deviation from the Arrhenius law in the sense that the dynamics are too fast. We surmise that the dominant effect at low frequencies, drive amplitudes, and temperatures becomes thermally assisted quantum tunneling, with perhaps a role for stochastic synchronization effects (*19*, *20*) in defining the sharp, but nonetheless temperature-dependent, low-frequency cutoff (Fig. 1).

The size of the clusters can be derived from the dependence of the magnetization on external magnetic field. The saturation of the magnetic response in Fig. 2A follows the familiar Brillouin form for Ising spins, $M \sim \tanh(mh_{ac}/k_BT)$. Unlike a simple paramagnet, m here is not the magnetic moment of a single Ho ion (*21*, *22*) but rather the total moment of the spins locked together in the cluster. Analysis of this nonlinear response reveals that the clusters responsible for the saturation and hole burning effects at $T = 0.110$ K and $f = 5$ Hz contain approximately 260 spins. This corresponds to cluster dimensions of approximately six Ho-Ho spacings on a side and a probability of cluster membership of 1% for any given spin in the crystal, comparable to that deduced from the spectral weight carved out by the hole. A cluster of 260 spins, each carrying 7 μ_B and driven at $h_{ac} = 0.5$ Oe, sets an effective energy scale $\sim$ 0.13 K, comparable to the measuring temperature T, the onset temperature for deviations from Arrhenius behavior and the temperature at which the spectral gap opens.

Beyond the implications for the problem of disordered magnets, our data demonstrate the ability to imprint phase-coherent information in a chemically homogeneous bulk magnetic material, using frequency as a label. This means that solid magnets may yet have a future in quantum information processing applications where coherent spin oscillations are actively manipulated to implement computations (*23*). The necessary next step would involve entangling the states, a possibility that can be explored in $Li(Ho,Y)F_4$, because for this material an external transverse field readily produces quantum mixing (*16*, *24*).

References and Notes

1. J. M. Kikkawa, I. P. Smorchkova, N. Samarth, D. D. Awschalom, *Science* **277**, 1284 (1997).
2. J. M. Luttinger, L. Tisza, *Phys. Rev.* **70**, 954 (1947).
3. D. H. Reich *et al.*, *Phys. Rev. B* **42**, 4631 (1990).
4. D. H. Reich, T. F. Rosenbaum, G. Aeppli, *Phys. Rev. Lett.* **59**, 1969 (1987).
5. A. Aharony, M. J. Stephen, *J. Phys. C* **14**, 1665 (1981).
6. A pair of induction coils was used in a standard gradiometer configuration, and the magnetization oscillations were measured using a digital lock-in technique. For sufficiently small h_{ac}, the oscillation amplitude is linear in h_{ac} and the constant of proportionality is a complex number representing the magnetic susceptibility, $\chi(f) = \chi'(f) + i\chi''(f)$; the real and imaginary parts represent the in-phase and dissipative out-of-phase signals, respectively. Measuring frequencies f ranged between 0.1 and 100 kHz. Field amplitudes less than 0.05 Oe were required for linear response. The $LiHo_xY_{1-x}F_4$ material was chosen for its known purity and homogeneity. The lattice constants vary by less than 0.01% between $x = 0$ and 1, helping ensure a statistically random distribution of the Ho ions. We have explicitly ruled out chemical segregation effects on the basis of neutron scattering studies, which find no evidence for nuclear short-range order due to clustering.
7. P. Debye, *Polar Molecules* (Chemical Catalogue, New York, 1929), p. 90.
8. P. K. Dixon, L. Wu, S. R. Nagel, B. D. Williams, J. P. Carini, *Phys. Rev. Lett.* **65**, 1108 (1990).
9. Long-time relaxation in dielectric glasses has been attributed to the opening of a dipole gap [D. J. Salvino, S. Rogge, B. Tigner, D. D. Osheroff, *Phys. Rev. Lett.* **73**, 268 (1994)].
10. A. L. Burin, *J. Low Temp. Phys.* **100**, 309 (1995).
11. See, for example, W. E. Moerner, Ed., *Persistent Spectral Hole Burning: Science and Applications* (Springer-Verlag, New York, 1988).
12. B. Scheiner, R. Bohmer, A. Loidl, R. V. Chamberlin, *Science* **274**, 752 (1996).
13. R. V. Chamberlin, *Phys. Rev. Lett.* **83**, 5134 (1999).
14. L. C. Cugliandolo, J. L. Iguain, *Phys. Rev. Lett.* **85**, 3448 (2000).
15. For a discussion of ringing oscillations in charge-density-wave systems, see S. N. Coppersmith and P. B. Littlewood [*Phys. Rev. B* **31**, 4049 (1985)].
16. J. Brooke, T. F. Rosenbaum, G. Aeppli, *Nature* **413**, 610 (2001).
17. K. Binder, A. P. Young, *Rev. Mod. Phys.* **58**, 801 (1986).
18. J. A. Mydosh, *Spin Glasses: An Experimental Introduction* (Taylor & Francis, London, 1993).
19. L. Gammoitoni, P. Hanggi, F. Marchesoni, *Rev. Mod. Phys.* **70**, 223 (1998).
20. A. Simon, A. Libchaber, *Phys. Rev. Lett.* **68**, 3375 (1992).
21. R. Giraud, W. Wernsdorfer, A. M. Tkachuk, D. Mailly, B. Barbara, *Phys. Rev. Lett.* **87**, 57203 (2001).
22. P. E. Hansen, T. Johansson, R. Nevald, *Phys. Rev. B* **12**, 5315 (1976).
23. N. A. Gershenfeld, I. L. Chuang, *Science* **275**, 350 (1997).
24. W. Wu, B. Ellman, T. F. Rosenbaum, G. Aeppli, D. H. Reich, *Phys. Rev. Lett.* **67**, 2076 (1991).

25. We have benefited greatly from discussions with J. Brooke, P. Chandra, S. Coppersmith, and S. Girvin. The work at the University of Chicago was supported primarily by the Materials Research Science and Engineering Centers Program of NSF under award DMR-9808595.

11 February 2002; accepted 2 May 2002

Antibody-Based Bio-Nanotube Membranes for Enantiomeric Drug Separations

Sang Bok Lee,[1] David T. Mitchell,[1] Lacramioara Trofin,[1] Tarja K. Nevanen,[2] Hans Söderlund,[2] Charles R. Martin[1]*

Synthetic bio-nanotube membranes were developed and used to separate two enantiomers of a chiral drug. These membranes are based on alumina films that have cylindrical pores with monodisperse nanoscopic diameters (for example, 20 nanometers). Silica nanotubes were chemically synthesized within the pores of these films, and an antibody that selectively binds one of the enantiomers of the drug was attached to the inner walls of the silica nanotubes. These membranes selectively transport the enantiomer that specifically binds to the antibody, relative to the enantiomer that has lower affinity for the antibody. The solvent dimethyl sulfoxide was used to tune the antibody binding affinity. The enantiomeric selectivity coefficient increases as the inside diameter of the silica nanotubes decreases.

Drugs that are produced as racemic mixtures normally contain only one enantiomer that is efficacious (*1*), and there is increasing pressure on the pharmaceutical industry to market enantiomerically pure drugs (*2*). One approach for obtaining an enantiomerically pure drug is to effect a chiral separation, typically by means of a chromatographic method (*3*, *4*). An alternative enantioseparation strategy entails the use of a synthetic membrane to selectively transport the desired enantiomer from the racemic mixture into a receiver solution on the other side of the membrane (*5*–*10*). This requires that an enantioselective molecular recognition agent be incorporated into the membrane, and there are a

[1]Department of Chemistry and Center for Research at the Bio/Nano Interface, University of Florida, Gainesville, FL 32611–7200, USA. [2]VTT Biotechnology, Post Office Box 1500, FIN-02044 VTT, Espoo, Finland.

*To whom correspondence should be addressed. E-mail: crmartin@chem.ufl.edu

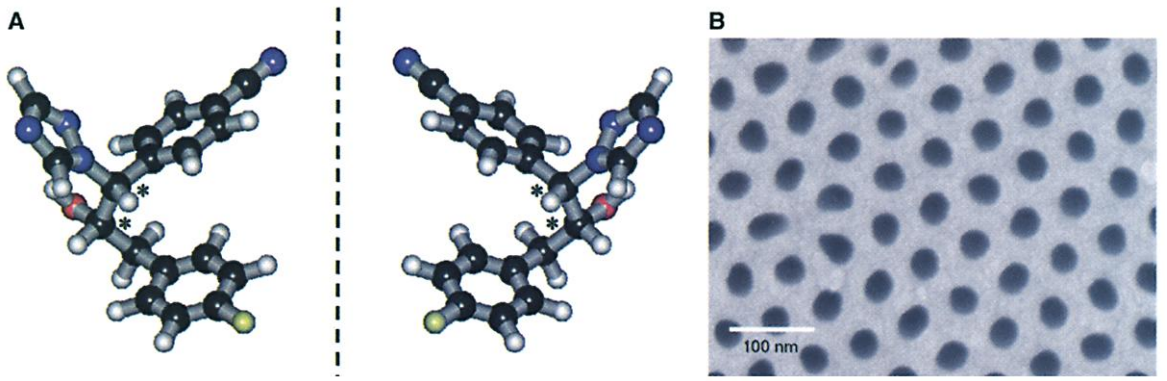

Fig. 1. (**A**) Three-dimensional structures of the drug enantiomers: RS enantiomer (left) and SR enantiomer (right). The black, white, blue, red, and yellow balls represent carbon, hydrogen, nitrogen, oxygen, and fluoride, respectively; asterisks denote the chiral centers. The geometry optimization was done by ab initio calculation with minimal basis set in HyperChem 6.03. The drug is in clinical trials by Hormos Medical Corporation, Turku, Finland. (**B**) Scanning electron micrograph of the surface of the alumina membrane with pores 35 nm in diameter before sol-gel synthesis of the silica nanotubes. These alumina membranes were 40 μm thick with a pore density of 2.1×10^{10} cm^{-2}.

few papers in the current literature on using molecular recognition proteins (such as enzymes) for this purpose (*8–10*).

Antibodies are perhaps the most specific of the molecular recognition proteins, and although they have been used in chromatographic experiments to perform enantio- and other bioseparations (*4*, *11*, *12*), there appear to be no examples of their use in membrane-permeation enantioseparations. This is perhaps because the binding constants for antibodies are often so large (*11*, *13–18*) that the binding event is essentially irreversible. This is undesirable because the membrane must ultimately release the target molecule so that it can be collected in the receiver solution. We show here that the binding affinity in synthetic nanotube membranes (*19*, *20*) that contain an enantioselective antibody can be chemically tuned by addition of dimethyl sulfoxide (DMSO) to the racemic and receiver solutions (*21*). These membranes effect chiral separations by selectively transporting the enantiomer that binds to the antibody relative to the enantiomer that has lower affinity for the antibody.

The antibodies were selected to bind the drug 4-[3-(4-fluorophenyl)-2-hydroxy-1-[1,2,4]triazol-1-yl-propyl]-benzonitrile (Fig. 1A), an inhibitor of aromatase enzyme activity (*4*). This molecule has two chiral centers and thus four stereoisomers: RR, SS, SR, and RS. The antibody used selectively binds the RS relative to the SR enantiomer, and membranes based on the Fab fragment (*4*, *13*, *22*) of this antibody were used to separate this enantiomeric pair. The cloning, production, and purification of this RS-enantiospecific Fab fragment (anti-RS) have been reported previously (*4*).

Nanopore alumina films (*23–25*) (Fig. 1B) were used as host membranes for immobilization of the anti-RS. Films having pores with diameters of 20 and 35 nm were used for these studies. A sol-gel template synthesis method was used to deposit silica nanotubes (with a wall thickness of <3 nm) within the pores of the alumina films (*23*, *26*). The inside walls of the silica nanotubes were then reacted with a silane that terminated in an aldehyde functional group (*27*). Aldehyde groups react spontaneously with free amino sites on proteins (*28–30*), and this approach was used to attach the anti-RS to the inside walls of the silica nanotubes (*31*).

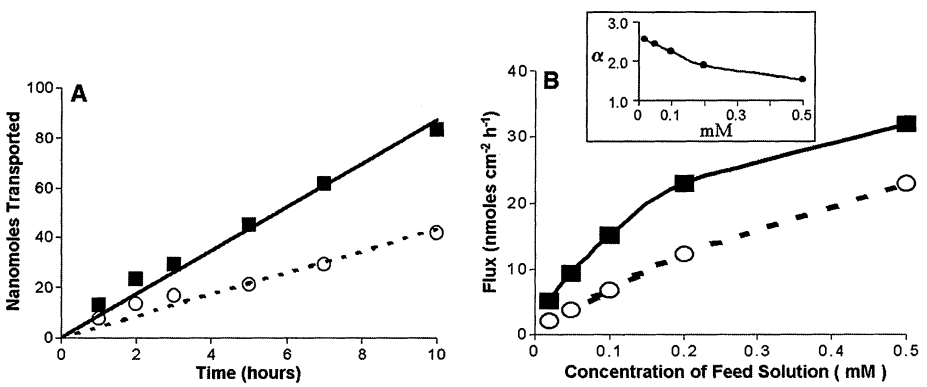

Fig. 2. (**A**) Plots of nanomoles of RS enantiomer (solid squares, solid line) and SR enantiomer (open circles, dashed line) transported from the feed solution into the permeate solution versus time through a silica nanotube alumina membrane modified with the anti-RS Fab fragment. The membrane had pores 35 nm in diameter. The feed solution was 0.1 mM in both the RS and SR enantiomers dissolved in 10% DMSO–phosphate-buffered saline (PBS) buffer (pH 8.5). (**B**) Plots of RS enantiomer (solid squares, solid line) and SR enantiomer (open circles, dashed line) flux versus concentration of the enantiomers in the feed solution for the membrane in (A). The buffer in this case was 15% in DMSO. The inset shows the dependence of the selectivity coefficient α on the feed concentration.

The anti-RS–containing membrane was mounted between the two halves of a U-tube permeation cell (*10*, *32–34*). A feed solution that was a racemic mixture of the RS and SR enantiomers (typically 0.1 mM in each enantiomer dissolved in pH = 8.5 phosphate buffer that was 10% in DMSO) was placed on one side of the membrane. The receiver solution on the other side of the membrane was just the phosphate/DMSO buffer. The fluxes of the RS and SR enantiomers across the membrane were determined by periodically assaying for these enantiomers in the receiver solution using a chiral high-performance liquid chromatography method (*35*).

The slopes of straight-line plots of moles transported versus time (Fig. 2A) provide the fluxes of the RS and SR enantiomers across the anti-RS–containing nanotube membrane. The ratio of the RS flux to the SR flux is the transport selectivity coefficient α. An average α value of 2.0 ± 0.2 was obtained for three identical membranes prepared from the alumina with a pore diameter of 35 nm, indicating that these membranes transport the RS enantiomer twice as fast as they transport the SR enantiomer. The same α value was obtained after storage of the membrane for 1 week in the phosphate/DMSO buffer.

Because it is the RS enantiomer that specifically binds to the immobilized anti-RS, these data suggest that this Fab fragment is facilitating (*10*, *36–41*) the transport of this enantiomer. If this is correct, theory predicts that the RS flux should initially increase linearly with feed concentration and that the curve of flux versus feed concentration should then flatten at higher concentrations (*10*). We investigated the effect of the con-

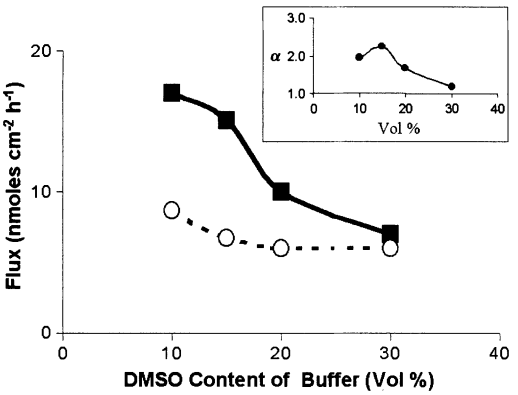

Fig. 3. Plots of RS enantiomer (solid squares, solid line) and SR enantiomer (open circles, dashed line) flux versus DMSO content in the buffer solution for the membrane in Fig. 2. The feed solution was 0.1 mM in each enantiomer. The inset shows the dependence of the selectivity coefficient α on the DMSO content of the buffer solution.

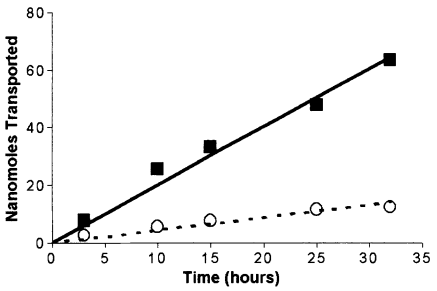

Fig. 4. Plots as per Fig. 2, but with an alumina membrane with pores 20 nm in diameter. The feed solution was 0.1 mM in each enantiomer dissolved in15% DMSO-PBS (pH 8.5). These alumina membranes were 35 μm thick, with a pore density of 2.3×10^{10} cm^{-2}.

centration of the enantiomers in the racemic feed solution on the fluxes (Fig. 2B) and observed this Langmuirian-shaped curve for the RS enantiomer. The plot for the SR enantiomer is more linear, although some curvature is observed at the highest concentrations, which suggests that this enantiomer interacts weakly with the anti-RS. Facilitated transport theory also predicts that the highest selectivity coefficient should be obtained at the lowest feed concentration, and this result was also observed (Fig. 2B, inset). A maximum selectivity coefficient of $\alpha = 2.6$ was obtained for this membrane.

Column chromatography experiments showed that the binding strength between the RS enantiomer and the anti-RS decreased with increasing DMSO content of the buffer (*4*, *21*). If the facilitated transport mechanism is operative, these data would suggest that the RS flux would be highest at low DMSO contents and that the flux would decrease with increasing DMSO content. Furthermore, the RS flux should ultimately become equal to the SR flux, because at high DMSO content, neither enantiomer interacts appreciably with the anti-RS (*4*, *21*). These predictions were observed experimentally (Fig. 3). The weak interaction of the SR enantiomer with anti-RS was also confirmed by these studies, because the SR flux shows a slight decrease with increasing DMSO content. These studies also illustrate that there is an optimal DMSO content that maximizes the value of the selectivity coefficient (Fig. 3, inset).

The selectivity in a facilitated transport process can be increased by shutting down the nonfacilitated (diffusional) transport of the unwanted chemical species; in porous membranes, this can be accomplished by decreasing the pore size in the membrane (*10*, *42*–*44*). We explored this issue by measuring RS versus SR flux in analogous membranes prepared with alumina films having pores 20 nm in diameter (Fig. 4). The selectivity coefficient increased to $\alpha = 4.5$ for this smaller pore-diameter membrane. However, as would be expected, the fluxes for both enantiomers were lower in the smaller pore-diameter membrane.

Because, in principle, antibodies can be obtained that selectively bind to any desired molecule or enantiomer, the concepts presented here might provide a general approach for obtaining selectively permeable membranes for a host of enantio- and bioseparations. However, throughput (that is, flux) in a membrane separation process is just as important as selectivity, and methods for enhancing flux across such membranes need to be developed. As per our prior work, this can be accomplished by making an ultrathin film composite (*45*) and/or by augmenting diffusive flux with pressure-driven (*46*) or electroosmotic (*19*) transport.

References and Notes

1. J. Crosby, *Tetrahedron* **47**, 4789 (1991).
2. P. E. M. Overdevest *et al.*, in *Surfactant-Based Separations*, J. F. Scamehorn, J. H. Harwell, Eds. (American Chemical Society, Washington, DC, 1999), chap. 9.
3. T. J. Ward, *Anal. Chem.* **72**, 4521 (2000).
4. T. K. Nevanen *et al.*, *J. Chromatogr. A* **925**, 89 (2001).
5. T. Aoki, M. Ohshima, K. I. Shinihara, T. Kaneko, E. Oikawa, *Polymer* **38**, 235 (1997).
6. S. Tone, T. Masawaki, K. Eguchi, *J. Membr. Sci.* **118**, 31 (1996).
7. M. Yoshikawa, J. I. Izumi, T. Kitao, S. Sakamoto, *Macromolecules* **29**, 8197 (1996).
8. A. Higuchi, M. Hara, T. Horiuchi, T. Nakagawa, *J. Membr. Sci.* **93**, 157 (1994).
9. M. Nakamura, S. Kiyohara, K. Saito, K. Sugita, T. Sugo, *J. Chromatogr. A* **822**, 53 (1998).
10. B. B. Lakshmi, C. R. Martin, *Nature* **388**, 758 (1997).
11. H. A. Chase, *Chem. Eng. Sci.* **39**, 1099 (1984).
12. K. Kojima, *J. Biochem. Biophys. Methods* **49**, 241 (2001).
13. E. Harlow, D. Lane, *Antibodies* (Cold Spring Harbor Laboratory Press, Cold Spring Harbor, NY, 1988), pp. 8–22.
14. A. Hemminki *et al.*, *Protein Eng.* **11**, 311 (1998).
15. P. S. Chowdhury, I. Pastan, *Nature Biotechnol.* **17**, 568 (1999).
16. A. Hemminki, S. Niemi, L. Hautoniemi, H. Söderlund, K. Takkinen, *Immunotechnology* **4**, 59 (1998).
17. D. E. Yelton *et al.*, *J. Immunol.* **155**, 1994 (1995).
18. M. Nachman, *J. Chromatogr.* **597**, 167 (1992).
19. S. A. Miller, V. Y. Young, C. R. Martin, *J. Am. Chem. Soc.* **123**, 12335 (2001).
20. K. B. Jirage, J. C. Hulteen, C. R. Martin, *Science* **278**, 655 (1997).
21. The effect of DMSO on the binding affinity for this antibody was demonstrated with column chromatography experiments (*4*). Buffers with low DMSO content (2%) resulted in essentially irreversible binding of the hapten to the antibody, and buffers with high DMSO content (>30%) destroyed the antibody-hapten interaction.
22. C. K. Mathews, K. E. Van Holde, *Biochemistry* (Benjamin/Cummings, Menlo Park, CA, 1996), pp. 247–249.
23. B. B. Lakshmi, C. J. Patrissi, C. R. Martin, *Chem. Mater.* **9**, 2544 (1997).
24. C. A. J. Foss, G. L. Hornyak, J. A. Stockert, C. R. Martin, *J. Phys. Chem.* **98**, 2963 (1994).
25. H. Masuda, M. Satoh, *Jpn. J. Appl. Phys. Part 2* **35** (no. 1B), L126 (1996).
26. C. J. Brinker, G. W. Scherer, *Sol-Gel Science* (Academic Press, New York, 1990).
27. Freshly made alumina membranes containing SiO_2 nanotubes were immersed into an ethanol-based solution that was 5% in aqueous acetate buffer and 10% in trimethoxysilylpropyl aldehyde (PSX1050, United Chemical Technologies, Bristol, PA); the pH was adjusted to 5.0. The resulting aldehyde-modified membranes were then rinsed with ethanol and dried for 24 hours in an Ar-filled (oxygen-free) glove box.
28. C. Bruning, J. Grobe, *Chem. Commun.* **1995**, 2323 (1995).
29. S. Wolpert, *J. Membr. Sci.* **132**, 23 (1997).
30. D. Stubbings, M. O. Bubb, J. D. Conradie, *Anal. Biochem.* **210**, 159 (1993).
31. The aldehyde-modified nanotube membranes were incubated overnight at 4°C and then for 1 day at room temperature with a solution of the Fab fragment in buffer (~2 mg of antibody per 1 ml of buffer). The antibody-modified membranes were then thoroughly rinsed with buffer solution before use. Although silanes also can be attached directly to the alumina pore walls, in preliminary experiments we found that membranes prepared without the silica nanotubes were less selective and had shorter lifetimes. Measurements of the amount of Fab fragment immobilized indicated that the average center-to-center distance between Fab fragment sites along the nanotube walls was ~17 nm. The Fab fragment had approximate dimensions of 3.5 nm by 5.5 nm by 6.0 nm.
32. M. Nishizawa, V. P. Menon, C. R. Martin, *Science* **268**, 700 (1995).
33. H. Bayley, C. R. Martin, *Chem. Rev.* **100**, 2575 (2000).
34. S. B. Lee, C. R. Martin, *Chem. Mater.* **13**, 3236 (2001).
35. The column used was an Ultron ES-OVM at 30°oC. The mobile phase was 20 mM ammonium phosphate (pH 5.0)-20% methanol (v/v) at a flow rate of 1.0 ml/min. The detection wavelength was 230 nm.
36. R. D. Noble, *J. Membr. Sci.* **75**, 121 (1992).
37. M.-F. Paugam *et al.*, *J. Am. Chem. Soc.* **118**, 9820 (1996).
38. P. R. Westmark, S. J. Gardiner, B. D. Smith, *J. Am. Chem. Soc.* **118**, 11093 (1996).
39. C. K. Kim *et al.*, *J. Phys. Chem. A* **105**, 9024 (2001).
40. Y. S. Park, J. Won, Y. S. Kang, *Langmuir* **16**, 9662 (2000).
41. J. Yang, P. Huang, *Chem. Mater.* **12**, 2693 (2000).
42. A. Javaid, M. P. Hughey, V. Varutbangkul, D. M. Ford, *J. Membr. Sci.* **187**, 141 (2001).
43. S. B. Lee, C. R. Martin, *Anal. Chem.* **73**, 768 (2001).
44. J. C. Hulteen, K. B. Jirage, C. R. Martin, *J. Am. Chem. Soc.* **120**, 6603 (1998).
45. C. Liu, C. R. Martin, *Nature* **352**, 50 (1991).
46. S. Yu, S. B. Lee, M. Kang, C. R. Martin, *Nano Lett.* **1**, 495 (2001).

47. Supported by NSF, the Office of Naval Research, and the National Technology Agency, Finland.

28 February 2002; accepted 26 April 2002